

Can a strong radio burst escape the magnetosphere of a magnetar?

ANDREI M. BELOBORODOV^{1,2}

¹*Physics Department and Columbia Astrophysics Laboratory, Columbia University, 538 West 120th Street, New York, NY 10027, USA*

²*Max Planck Institute for Astrophysics, Karl-Schwarzschild-Str. 1, D-85741, Garching, Germany*

ABSTRACT

We examine the possibility that fast radio bursts (FRBs) are emitted inside the magnetosphere of a magnetar. On its way out, the radio wave must interact with a low-density e^\pm plasma in the outer magnetosphere at radii 10^9 - 10^{10} cm. In this region, the magnetospheric particles have a huge cross section for scattering the wave. As a result, the wave strongly interacts with the magnetosphere and compresses it, depositing the FRB energy into the compressed field and the scattered radiation. The scattered spectrum extends to the γ -ray band and triggers e^\pm avalanche, further boosting the opacity. These processes choke FRBs, excluding emission of observed bursts from radii $R \ll 10^{10}$ cm.

Keywords: Neutron stars (1108); Magnetars (992); Radiative processes (2055); Radio bursts (1339)

1. INTRODUCTION

Fast radio bursts (FRBs) are a big puzzle. They are detected from cosmological distances with luminosities up to 10^{43} erg/s and ms durations (Petroff et al. 2019). Spectacular progress in FRB observations, in particular by CHIME, has provided a wealth of data which miss theoretical explanation. Recent FRB detection from SGR 1935+2154 (The CHIME/FRB Collaboration et al. 2020; Bochenek et al. 2020) supports the association of FRBs with magnetars. However, their emission mechanism is not established. Possible scenarios are (1) emission near the magnetar, inside its ultrastrong magnetosphere (“near-field”) and (2) emission at much larger radii from explosions launched by magnetospheric flares into the magnetar wind (“far-field”). The far-field models include a robust radiative mechanism—synchrotron maser emission from the blast wave (Lyubarsky 2014; Beloborodov 2017, 2020; Metzger et al. 2019; Sironi et al. 2021) and possible emission from the magnetic flare ejecta (Lyubarsky 2020). On the other hand, it was argued that the observed temporal structure of FRBs favors the near-field scenario (The CHIME/FRB Collaboration et al. 2021; Nimmo et al. 2021).

Cosmological FRBs are 10^{10} - 10^{12} times brighter than radio pulsations detected in several magnetars (Kaspi & Beloborodov 2017). Proposals for magnetospheric radio emission (Thompson 2008; Beloborodov 2013a; Lu et al. 2020; Lyutikov 2021) face serious challenges when applied to FRBs (Lyubarsky 2021).

An important requirement for a near-field FRB scenario is the successful escape of the radio wave. The wave must propagate through the plasma in the closed magnetosphere, which extends to the light cylinder

$$R_{\text{LC}} = \frac{c}{\Omega} \approx 5 \times 10^9 \left(\frac{P}{1 \text{ s}} \right) \text{ cm}, \quad (1)$$

where $P = 2\pi/\Omega$ is the rotation period of the magnetar. The plasma is immersed in the magnetospheric field B_{bg} and has gyro-frequency

$$\omega_B = \frac{eB_{\text{bg}}}{m_e c} \approx \frac{e\mu}{m_e c R^3} \approx 1.8 \times 10^{13} \frac{\mu_{33}}{R_9^3} \text{ rad/s}, \quad (2)$$

where e and m_e are the electron charge and mass, and the magnetic dipole moment $\mu = B_{\text{bg}} R^3 \sim 10^{33} \text{ G cm}^3$ corresponds to a surface magnetic field $B_* \sim 10^{15} \text{ G}$. The radio wave frequency $\nu = \omega/2\pi \sim 1 \text{ GHz}$ satisfies $\omega < \omega_B$ at all radii up to R_{LC} if $P < 3 \mu_{33}^{1/2} \text{ s}$.

The magnetosphere is normally assumed to be transparent to waves polarized perpendicular to the background magnetic field \mathbf{B}_{bg} , especially if $\omega \ll \omega_B$. A standard calculation of the electron cross section for wave scattering gives $\sigma_{\text{sc}} \approx (\omega/\omega_B)^2 \sigma_{\text{T}} \ll \sigma_{\text{T}}$ (Canuto et al. 1971) where σ_{T} is the Thomson cross section.

However, the small σ_{sc} holds only for wave amplitudes $E_0 < B_{\text{bg}}$. In fact, as the wave propagates away from the magnetar in the decreasing background $B_{\text{bg}} \propto R^{-3}$, its amplitude $E_0 \propto R^{-1}$ exceeds B_{bg} :

$$\frac{E_0}{B_{\text{bg}}} = \left(\frac{R}{R_0} \right)^2, \quad R_0 \approx 3.5 \times 10^8 \frac{\mu_{33}^{1/2}}{L_{42}^{1/4}} \text{ cm}, \quad (3)$$

where $L = cR^2 E_0^2/2$ is the isotropic equivalent of the FRB luminosity. Hereafter we focus on the wave propagation at radii $R > R_0$ where $E_0 > B_{\text{bg}}$. This condition is equivalent to $a_0 > \omega_B/\omega$, where

$$a_0 = \frac{eE_0}{m_e c \omega} \approx 2.3 \times 10^4 \frac{L_{42}^{1/2}}{R_9 \nu_9}. \quad (4)$$

Waves with $E_0 > B_{\text{bg}}$ are scattered with σ_{sc} exceeding σ_{T} by many orders of magnitude (Beloborodov 2021,

hereafter B21). Particles (e^\pm) exposed to the wave are quickly accelerated to huge Lorentz factors, exceeding 10^4 , and emit γ -rays capable of e^\pm creation. Below we examine implications of these processes for FRBs. For definiteness we consider a plane wave propagating perpendicular to \mathbf{B}_{bg} ; for different propagation angles $\theta \neq \pi/2$ one should replace $\omega_B \rightarrow \omega_B \sin \theta$.

2. SCATTERING OF THE WAVE

2.1. Magnetospheric plasma density n_0

The scattering opacity of the magnetosphere depends on its initial plasma density n_0 before it is exposed to the outgoing ultrastrong wave. One characteristic density in the problem is $n_{\text{co}} = |\nabla \cdot \mathbf{E}_{\text{co}}|/4\pi e$, the minimum needed to sustain the co-rotation electric field $\mathbf{E}_{\text{co}} = \mathbf{B}_{\text{bg}} \times (\boldsymbol{\Omega} \times \mathbf{R})$ (Goldreich & Julian 1969),

$$n_{\text{co}} \sim \frac{\mu}{ceR^3P} \approx 7 \times 10^4 \frac{\mu_{33}}{R_9^3} \left(\frac{P}{1\text{ s}}\right)^{-1} \text{ cm}^{-3}. \quad (5)$$

As shown below, even this low density is sufficient to choke FRBs emitted at $R \ll R_{\text{LC}}$.

The actual density around active magnetars is higher than n_{co} . The e^\pm plasma is created near the neutron star, at a radius $R_\pm \lesssim 10R_*$, and fills the outer magnetosphere by flowing out along the extended magnetic field lines. The particle flow at a radius $R \gg R_\pm$ scales with the number of field lines connecting R_\pm and R : $\dot{N}(R) \propto R^{-1}$ (Beloborodov 2020).

The value of \dot{N} may be estimated using observations of known magnetars in our galaxy. Their typical persistent luminosity in the keV band is $L_{\text{keV}} \sim 10^{35}$ erg/s, and the spectrum at higher photon energies carries $\sim 10^{36}$ erg/s (Kaspi & Beloborodov 2017). The spectrum is emitted by the e^\pm flow, which radiates its energy via resonant cyclotron scattering (Thompson et al. 2002; Beloborodov 2013b). The keV radiation is emitted by particles reaching $R_{\text{keV}} \sim 2 \times 10^7 \mu_{33}^{1/3}$ cm ($\hbar\omega_B \sim 1$ keV), and the flow decelerates to a mildly relativistic speed at $R \sim R_{\text{keV}}$. This implies e^\pm supply to R_{keV} with rate $\dot{N}(R_{\text{keV}}) \sim L_{\text{keV}}/m_e c^2$. This estimate is also consistent with the theoretically expected multiplicity of e^\pm production around magnetars (Beloborodov 2013b).

Then, using the scaling $\dot{N}(R) \propto R^{-1}$, one can estimate the e^\pm density in the outer magnetosphere as

$$n_0(R) \sim \frac{\dot{N}(R)}{cR^2} \sim 10^{10} R_9^{-3} \left(\frac{L_{\text{keV}}}{10^{35} \text{ erg/s}}\right) \text{ cm}^{-3}. \quad (6)$$

Note that Eqs. (5) and (6) both give a density $\propto R^{-3}$. Therefore, a convenient density parameter is

$$\mathcal{N} \equiv n_0 R^3. \quad (7)$$

Eqs. (5) and (6) give $\mathcal{N} \sim 10^{32}$ and 10^{37} , respectively.

2.2. Bulk acceleration and compression

Larmor rotation of particles in B_{bg} effectively couples the plasma to the background magnetic field lines. On scales larger than the Larmor scale, the plasma behaves as an MHD fluid. Before discussing the scattering opacity, it is useful to look at the MHD response of the magnetosphere to the force exerted by wave scattering.

The basic response is the sudden bulk acceleration and compression of the magnetosphere. The MHD coupling implies that the momentum received by the plasma from wave scattering is shared with the background field, so there appears an outward Poynting flux $\mathbf{S}_{\text{bg}} = (c/4\pi)\hat{\mathbf{E}}_{\text{bg}} \times \hat{\mathbf{B}}_{\text{bg}}$ and the magnetic field lines begin to drift with speed $\beta_{\text{bg}} = \hat{E}_{\text{bg}}/\hat{B}_{\text{bg}}$. Here, $\hat{\mathbf{E}}_{\text{bg}}$ and $\hat{\mathbf{B}}_{\text{bg}}$ are the new values of the background field, changing from the pre-wave values \mathbf{B}_{bg} and $\mathbf{E}_{\text{bg}} = 0$. In the ideal MHD approximation, the plasma and the background field drift with equal speed,

$$\beta_p = \beta_{\text{bg}} = \frac{\hat{E}_{\text{bg}}}{\hat{B}_{\text{bg}}}. \quad (8)$$

Acceleration to β_p is accompanied by compression,

$$\frac{\hat{B}_{\text{bg}}}{B_{\text{bg}}} = \frac{n}{n_0} = \frac{1}{1 - \beta_p}. \quad (9)$$

The wave compresses the magnetosphere of radius R into a shell of thickness $\sim (1 - \beta_p)R$.

Let τ_{sc} be the scattering optical depth encountered by the wave as it propagates to a radius R , and suppose $\tau_{\text{sc}} < 1$. Since the magnetosphere is magnetically dominated, the momentum lost by the wave $\tau_{\text{sc}}\mathcal{E}/c$ is mostly taken by the background field:

$$(1 - \beta_p)R \frac{S_{\text{bg}}}{c^2} \sim \frac{\tau_{\text{sc}}\mathcal{E}}{4\pi R^2 c}, \quad (10)$$

where $S_{\text{bg}}/c^2 = \beta_p \hat{B}_{\text{bg}}^2/4\pi c$ is the momentum density of the background field. This gives the equation for β_p ,

$$\frac{\beta_p}{1 - \beta_p} \sim \frac{\tau_{\text{sc}}\mathcal{E}}{R^3 B_{\text{bg}}^2} \sim \tau_{\text{sc}} R_9^3 \frac{\mathcal{E}_{39}}{\mu_{33}^2}. \quad (11)$$

One can see that any significant scattering at $R > 10^9$ cm is accompanied by sweeping the outer magnetosphere to a high Lorentz factor $\gamma_p = (1 - \beta_p^2)^{-1/2}$. This bulk acceleration must be self-consistently taken into account when calculating the wave scattering.

The wave has a small duration $T \sim 1$ ms $\ll R/c$. The compressed magnetospheric shell crosses the wave and exits behind it on the timescale $t_{\text{cross}} = T/(1 - \beta_p)$. As long as $t_{\text{cross}} < R/c$, the plasma is not stuck in a leading portion of the wave, and the entire wave interacts with the plasma. The condition $t_{\text{cross}} < R/c$ is satisfied at

$$R < R_{\text{surf}} \sim 6 \times 10^9 \tau_{\text{sc}}^{-1/2} \mathcal{E}_{39}^{-1/2} T_{-3}^{-1/2} \mu_{33} \text{ cm}. \quad (12)$$

For typical parameters, R_{surf} is comparable to R_{LC} , and $t_{\text{cross}} < R/c$ is satisfied in the entire magnetosphere.

2.3. Scattering optical depth

For a successfully escaping wave, the net energy lost to scattering \mathcal{E}_{sc} must be small compared with the wave energy $\mathcal{E} = LT = 4\pi R^2 FT$, where $F = cE_0^2/8\pi$ is its energy flux. The lost energy fraction may be written as

$$\tau_{\text{sc}} = \frac{\mathcal{E}_{\text{sc}}}{\mathcal{E}} \sim n_0 R \sigma'_{\text{sc}}, \quad (13)$$

where n_0 is the initial (pre-wave) plasma density, and σ'_{sc} is the scattering cross section of e^\pm measured in frame K' that moves with speed β_p (the rest frame of the accelerated and compressed magnetospheric shell).

Hereafter all quantities with primes refer to frame K' . In this frame, the background field is purely magnetic: $\mathbf{B}'_{\text{bg}} \neq 0$, $\mathbf{E}'_{\text{bg}} = 0$. The transformations of the wave frequency ω and field \hat{B}_{bg} to frame K' give

$$\omega' = \frac{\omega}{\gamma_p(1 + \beta_p)}, \quad \omega'_B = \frac{\hat{\omega}_B}{\gamma_p} = \gamma_p(1 + \beta_p)\omega_B. \quad (14)$$

Wave strength parameter $a'_0 = a_0$ is Lorentz invariant.

In frame K' , a minimum Lorentz factor developed by particles oscillating in the wave is $\gamma' \sim a_0$.¹ Each particle emits curvature radiation with power $\dot{\mathcal{E}}'_e = \dot{\mathcal{E}}_e$, which determines the effective scattering cross section $\sigma'_{\text{sc}} = \dot{\mathcal{E}}_e/F'$. To get an idea of the importance of scattering, one can start with a simple guess that particles in waves with $E'_0 \gg B'_{\text{bg}}$ emit similarly to the known result at $B'_{\text{bg}} = 0$: $\dot{\mathcal{E}}_e \sim e^2 \omega'^2 \gamma'^4 \sim e^2 \omega'^2 a_0^4$, which gives $\sigma'_{\text{sc}} \sim a_0^2 \sigma_{\text{T}}$ (Landau & Lifshitz 1975). Then, one finds

$$\tau_{\text{sc}} \sim \frac{\sigma'_{\text{sc}} \mathcal{N}}{R^2} \sim \frac{3 \times 10^3}{R_9^4} \frac{L_{42}}{\nu_9^2} \left(\frac{\sigma'_{\text{sc}}}{a_0^2 \sigma_{\text{T}}} \right) \mathcal{N}_{37}. \quad (15)$$

The actual effect of $B'_{\text{bg}} \ll E'_0$ on σ'_{sc} is not small and can give $\sigma'_{\text{sc}} \gg a_0^2 \sigma_{\text{T}}$ (Section 2.4). Furthermore, we will show that a low $n_0 \sim n_{\text{co}}$ ($\mathcal{N} \sim 10^{32}$) provides sufficient seeds for e^\pm avalanche, which again leads to $\tau_{\text{sc}} \gg 1$.

2.4. Scattering cross section

B21 calculated the particle motion in frame K' and found σ'_{sc} in two regimes (pink/olive regions in Fig. 1):

(I) If $\omega'_B < \omega'$, the particle motion is dominated by the ω' -oscillations in the wave. Then,

$$\frac{\sigma'_{\text{sc}}}{a_0^2 \sigma_{\text{T}}} \approx \begin{cases} 1 & a_0 < a'_1 \\ (a_0/a_1)^{-0.6} & a_0 > a'_1 \end{cases} \quad (16)$$

$$a'_1 \equiv \left(\frac{c}{r_e \omega'} \right)^{1/4} \sim 3 \times 10^3, \quad r_e \equiv \frac{e^2}{m_e c^2}. \quad (17)$$

¹ The high $\omega'_B > \omega'$ does not prevent the particle acceleration by $E'_0 \gg B'_{\text{bg}}$ — the strong wave changes the particle's Lorentz factor by $\sim a_0$ before it completes one gyration in B'_{bg} . Effects of the background field are important on longer timescales, as gyration in B'_{bg} shapes the plasma bulk motion (Section 2.2) and also enables resonant pumping of $\gamma' \gg a_0$ (B21).

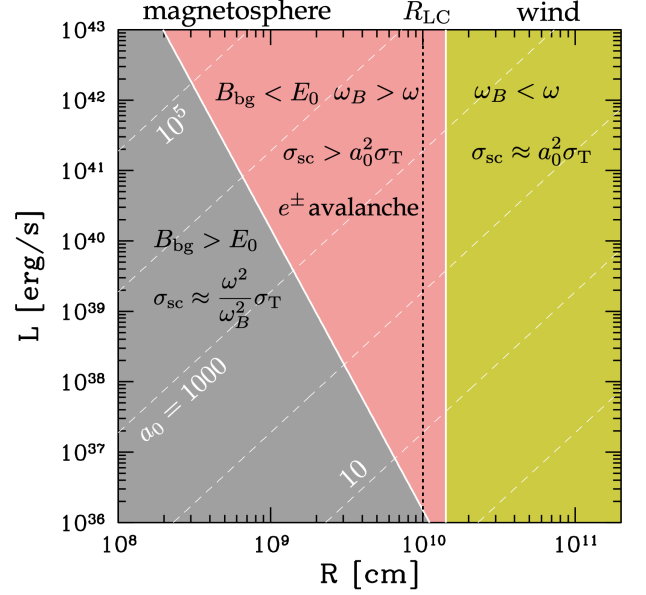


Figure 1. Three regions on the radius-luminosity plane for an FRB with $\nu = \omega/2\pi = 1$ GHz. The magnetar is assumed to have a magnetic dipole moment $\mu = 10^{33}$ G cm³ and spin period $P = 2$ s. In the region of $B_{\text{bg}} > E_0$ (grey), scattering is suppressed. In the region of $1 < \omega_B/\omega < a_0$ (pink), strong scattering and the avalanche of e^\pm creation occur, which choke the FRB. In the region of $\omega_B < \omega$ (olive), the scattering opacity quickly falls off. The $\omega_B = \omega$ boundary between scattering regimes I (olive) and II (pink) is shown in the limit of $n_0 \rightarrow 0$, $\beta_p = 0$ ($\sigma'_{\text{sc}} = \sigma_{\text{sc}}$). With increasing τ_{sc} , the plasma bulk acceleration expands the pink region.

(II) If $\omega'_B > \omega'$ and the wave has strength $a_0 < a'_* \approx (c\omega_B^2/r_e\omega'^3)^{1/5}$, the particle motion becomes simple Larmor rotation in B'_{bg} with frequency $\omega'_L = \omega'_B/\gamma' < \omega'$ (with superimposed subdominant ω' -oscillations in the wave). The Larmor rotation is pumped because the particle experiences a resonance with the wave every Larmor period, as explained in detail in B21. As a result, the particle's Lorentz factor is quickly pushed to the radiation reaction limit (RRL),

$$\gamma'_{\text{RRL}} \approx \left(\frac{c}{r_e \omega' a_0} \right)^{3/8} \left(\frac{\omega'_B}{\omega'} \right)^{1/4}, \quad (18)$$

and the resulting scattering cross section is

$$\frac{\sigma'_{\text{sc}}}{\sigma_{\text{T}}} \sim \gamma'^2_{\text{RRL}} \approx 2 \times 10^8 \frac{[\gamma_p(1 + \beta_p)]^{7/4} \mu_{33}^{1/2}}{R_9^{3/4} L_{42}^{3/8} \nu_9^{1/2}}. \quad (19)$$

The condition $a_0 < a'_*$ implies $\sigma'_{\text{sc}} \gg a_0^2 \sigma_{\text{T}}$; it is satisfied for most FRBs,

$$\frac{a'_*}{a_0} \approx \frac{\gamma_p(1 + \beta_p)}{2.3} \frac{\mu_{33}^{2/5} \nu_9^{2/5}}{R_9^{1/5} L_{42}^{1/2}}. \quad (20)$$

Note also that Eqs. (16) and (19) do not match at $\omega'_B = \omega'$; there is a sharp change of σ'_{sc} across this transition.

3. AVALANCHE OF PAIR CREATION

A magnetospheric particle exposed to the strong radio wave radiates the power $\dot{\mathcal{E}}_e = \sigma'_{\text{sc}} F'$ in photons with characteristic frequency $\omega'_c = (3/2)\gamma'^3 c/r'_c$, where $r'_c{}^{-1} = (3\dot{\mathcal{E}}_e/2ce^2\gamma'^4)^{1/2}$ is the curvature of the particle's trajectory. The corresponding energy $\epsilon'_c \equiv \hbar\omega'_c/m_e c^2$ is in the γ -ray band. Using the results of B21, we find in regime I:

$$\epsilon'_c \approx a_0^3 \frac{\hbar\omega'}{m_e c^2} \approx \frac{100}{\gamma_p(1+\beta_p)} \frac{L_{42}^{3/2}}{R_9^3 \nu_9^2}, \quad (21)$$

and in regime II:

$$\epsilon'_c \approx \frac{1}{\alpha} \left(\frac{r_e \omega_B^2 a_0}{c \omega'} \right)^{1/4} \approx 44 \frac{[\gamma_p(1+\beta_p)]^{3/4} \mu_{33}^{1/2} L_{42}^{1/8}}{R_9^{7/4} \nu_9^{1/2}}. \quad (22)$$

where $\alpha = e^2/\hbar c$. We conclude that the wave generates γ -rays with $\epsilon'_c \gg 1$. Their spectrum has a peak with a half-width extending from $0.01\epsilon'_c$ to $1.5\epsilon'_c$ (e.g. Longair 2011). This broad peak extends over the MeV band where photon-photon collisions $\gamma + \gamma \rightarrow e^+ + e^-$ occur with cross section $\sigma'_{\gamma\gamma} \sim 0.1\sigma_{\text{T}}$.

It is convenient to view e^\pm creation in frame K' , where the emitted γ -rays are quasi-isotropic.² The energy emitted as the wave expands to radius R , $\mathcal{E}'_{\text{sc}} = \mathcal{E}_{\text{sc}}/\gamma_p$, occupies radial thickness $\Delta R' \sim R/\gamma_p$, so the γ -rays have energy density

$$U'_\gamma \approx \frac{\tau_{\text{sc}} \mathcal{E}}{4\pi R^3}. \quad (23)$$

They exit behind the wave on a timescale comparable to the wave duration $T' = \gamma_p(1+\beta_p)T$, and a fraction of γ -rays convert to e^\pm pairs before exiting. The number of converting γ -rays per primary particle is

$$\mathcal{M}_\pm = \frac{\bar{\sigma}'_{\gamma\gamma} U'_\gamma c T'}{m_e c^2} \frac{\dot{\mathcal{E}}_e T'}{m_e c^2} \approx \zeta \frac{cT}{R} \frac{\sigma'_{\text{sc}}}{\sigma_{\text{T}}} \ell^2 \tau_{\text{sc}}, \quad (24)$$

where

$$\ell \equiv \frac{\sigma_{\text{T}} \mathcal{E}}{4\pi R^2 m_e c^2} \approx 66 \frac{\mathcal{E}_{39}}{R_9^2}, \quad (25)$$

and $\bar{\sigma}'_{\gamma\gamma} = \zeta \sigma_{\text{T}}$ is an effective cross section for $\gamma\gamma$ collisions. The numerical factor ζ may be found by integrating the $\gamma\gamma$ reaction rate over the spectrum of curvature emission. It depends on ϵ'_c and varies around $\zeta \sim 10^{-2}$ at radii where $\epsilon'_c > 1$.

The e^\pm created by γ -rays oscillate in the wave and emit secondary γ -rays just like the primary particles do. An avalanche of e^\pm creation develops if $\mathcal{M}_\pm \gg 1$, boosting the plasma density by $\exp \mathcal{M}_\pm$. One can see that

\mathcal{M}_\pm is large, even if one chooses a low density $n_0 = n_{\text{co}}$,

$$\mathcal{M}_\pm \sim \frac{10^8 \zeta}{R_9^7} \mathcal{E}_{39}^2 T_{-3}^2 \sigma_8^2 \mathcal{N}_{32} \gg 1. \quad (26)$$

where $\sigma_8 = \sigma'_{\text{sc}}/10^8 \sigma_{\text{T}}$. The wave becomes immersed in the exponentially enriched e^\pm plasma with $\tau_{\text{sc}} \gg 1$.

4. DISCUSSION

The values of $\tau_{\text{sc}} \gg 1$ found above assume no feedback of scattering on the wave. In reality, the wave strength must drop to satisfy $\tau_{\text{sc}} \lesssim 1$, respecting energy conservation $\mathcal{E}_{\text{sc}} \lesssim \mathcal{E}$. The condition $\tau_{\text{sc}}(L, R) \sim 1$ defines a minimum emission radius $R_{\text{min}}(L)$. Our results show that R_{min} is comparable to R_{LC} for cosmological FRBs. This constraint is based on established laws of electrodynamics and challenges the near-field interpretation of the FRB temporal structure observed by CHIME.

Interestingly, lowering L may not help the burst to escape from $R \ll 10^{10}$ cm, because $\sigma'_{\text{sc}} \propto L^{-3/8}$ grows at lower L (Eq. 19), and $\epsilon'_c \propto L^{1/8}$ weakly changes. The main helping effect of lowering L is the growth of $R_0 \propto L^{-1/4}$ (Eq. 3). When $L \lesssim 10^{36}$ erg/s, R_0 reaches $\sim 10^{10}$ cm, the zone of strong particle acceleration $1 < a_0 < \omega_B/\omega$ disappears, and the wave scattering practically vanishes. The FRBs detected from SGR 1935+2154 are close to this transition.

The presented calculations assume that the radio wave propagates with speed c . This is a good approximation. The wave dispersion relation in frame K' has the form $\omega'^2 = c^2 k'^2 + \omega_p'^2$ where $\omega_p'^2 \approx 4\pi e^2 n'/\gamma' m_e$ and $n' = \gamma_p(1+\beta_p)\tau_{\text{sc}}/R\sigma'_{\text{sc}}$ is the plasma density. The group speed $v'_{\text{gr}} = d\omega'/dk'$ has Lorentz factor $\gamma'_{\text{gr}} \approx \omega'/\omega'_p$. In regime II we find (using $\gamma' \sim \gamma'_{\text{RRL}}$ and $\sigma'_{\text{sc}} \sim \gamma'^2_{\text{RRL}} \sigma_{\text{T}}$)

$$\gamma'_{\text{gr}} \sim \frac{5 \times 10^3 \mu_{33}^{3/8} \nu_9^{5/8}}{\tau_{\text{sc}}^{1/2} [\gamma_p(1+\beta_p)]^{3/16} R_9^{1/16} L_{42}^{9/32}}. \quad (27)$$

Our calculations focused on the closed magnetosphere. In a similar way, one can evaluate τ_{sc} in the wind at $R \gg R_{\text{LC}}$, where $n_0 \sim \mathcal{N}/R_{\text{LC}} R^2$, $B_{\text{bg}} \approx \mu/R_{\text{LC}}^2 R$, and scattering occurs in regime I ($\omega'_B < \omega'$) with $\sigma'_{\text{sc}} \approx a_0^2 \sigma_{\text{T}}$. With increasing R , $\hbar\omega'_c \approx a_0^3 \hbar\omega'$ quickly falls below $m_e c^2$, so the additional e^\pm creation becomes exponentially suppressed, and one finds

$$\tau_{\text{sc}} \sim \frac{a_0^2 \sigma_{\text{T}} \mathcal{N}}{R_{\text{LC}} R} \approx \frac{0.7 L_{42} \mathcal{N}_{37}}{R_{10}^3 \nu_9^2 (P/1\text{s})} \quad (R > 10^{10} \text{ cm}). \quad (28)$$

In particular, τ_{sc} is negligible if the observed FRBs are emitted by blast waves in the magnetar wind, which generate coherent radio emission at $R \sim 10^{13} - 10^{14}$ cm, although *induced* scattering could still be important in this model (Beloborodov 2020).

I thank Yuri Levin for comments which helped improve the manuscript. This work is supported by NSF grant AST 2009453, Simons Foundation grant #446228, and the Humboldt Foundation.

REFERENCES

- Beloborodov, A. M. 2013a, *ApJ*, 777, 114, doi: [10.1088/0004-637X/777/2/114](https://doi.org/10.1088/0004-637X/777/2/114)
- . 2013b, *ApJ*, 762, 13, doi: [10.1088/0004-637X/762/1/13](https://doi.org/10.1088/0004-637X/762/1/13)
- . 2017, *ApJL*, 843, L26, doi: [10.3847/2041-8213/aa78f3](https://doi.org/10.3847/2041-8213/aa78f3)
- . 2020, *ApJ*, 896, 142, doi: [10.3847/1538-4357/ab83eb](https://doi.org/10.3847/1538-4357/ab83eb)
- . 2021, arXiv e-prints, arXiv:2108.05464. <https://arxiv.org/abs/2108.05464>
- Bochenek, C. D., Ravi, V., Belov, K. V., et al. 2020, *Nature*, 587, 59, doi: [10.1038/s41586-020-2872-x](https://doi.org/10.1038/s41586-020-2872-x)
- Canuto, V., Lodenquai, J., & Ruderman, M. 1971, *PhRvD*, 3, 2303, doi: [10.1103/PhysRevD.3.2303](https://doi.org/10.1103/PhysRevD.3.2303)
- Goldreich, P., & Julian, W. H. 1969, *ApJ*, 157, 869, doi: [10.1086/150119](https://doi.org/10.1086/150119)
- Kaspi, V. M., & Beloborodov, A. M. 2017, *ARA&A*, 55, 261, doi: [10.1146/annurev-astro-081915-023329](https://doi.org/10.1146/annurev-astro-081915-023329)
- Landau, L. D., & Lifshitz, E. M. 1975, *The classical theory of fields*
- Longair, M. S. 2011, *High Energy Astrophysics*
- Lu, W., Kumar, P., & Zhang, B. 2020, *MNRAS*, 498, 1397, doi: [10.1093/mnras/staa2450](https://doi.org/10.1093/mnras/staa2450)
- Lyubarsky, Y. 2014, *MNRAS*, 442, L9, doi: [10.1093/mnrasl/slu046](https://doi.org/10.1093/mnrasl/slu046)
- . 2020, *ApJ*, 897, 1, doi: [10.3847/1538-4357/ab97b5](https://doi.org/10.3847/1538-4357/ab97b5)
- . 2021, *Universe*, 7, 56, doi: [10.3390/universe7030056](https://doi.org/10.3390/universe7030056)
- Lyutikov, M. 2021, arXiv e-prints, arXiv:2102.07010. <https://arxiv.org/abs/2102.07010>
- Metzger, B. D., Margalit, B., & Sironi, L. 2019, *MNRAS*, 485, 4091, doi: [10.1093/mnras/stz700](https://doi.org/10.1093/mnras/stz700)
- Nimmo, K., Hessels, J. W. T., Kirsten, F., et al. 2021, arXiv e-prints, arXiv:2105.11446. <https://arxiv.org/abs/2105.11446>
- Petroff, E., Hessels, J. W. T., & Lorimer, D. R. 2019, *A&A Rv*, 27, 4, doi: [10.1007/s00159-019-0116-6](https://doi.org/10.1007/s00159-019-0116-6)
- Sironi, L., Plotnikov, I., Nättilä, J., & Beloborodov, A. M. 2021, *PhRvL*, 127, 035101, doi: [10.1103/PhysRevLett.127.035101](https://doi.org/10.1103/PhysRevLett.127.035101)
- The CHIME/FRB Collaboration, :, Andersen, B. C., et al. 2020, arXiv e-prints, arXiv:2005.10324. <https://arxiv.org/abs/2005.10324>
- The CHIME/FRB Collaboration, Andersen, B. C., Bandura, K., et al. 2021, arXiv e-prints, arXiv:2107.08463. <https://arxiv.org/abs/2107.08463>
- Thompson, C. 2008, *ApJ*, 688, 499, doi: [10.1086/592061](https://doi.org/10.1086/592061)
- Thompson, C., Lyutikov, M., & Kulkarni, S. R. 2002, *ApJ*, 574, 332, doi: [10.1086/340586](https://doi.org/10.1086/340586)

² In regime I with $a_0 > a'_1$, the emission has a backward beaming in frame K' ; however this regime is not relevant for most FRBs.